Geophysical Research Letters

RESEARCH LETTER
10.1029/2020GL088345

Characteristics of the Prolonged El Niño Events During 1960–2020

Chung-Wei Lee[1], Yu-Heng Tseng[2], Chung-Hsiung Sui[1], Fei Zheng[3], and Erh-Tung Wu[1]

[1]Department of Atmospheric Sciences, National Taiwan University, Taipei, Taiwan, [2]Institute of Oceanography, National Taiwan University, Taipei, Taiwan, [3]Institude of Atmospheric Physics, Chinese Academy of Sciences, Beijing, China

Key Points:
- Prolonged El Niño accounts for 5 out of the 17 El Niño events from 1960 to 2020
- The prolonged events show a slower evolution and develop late by about 3 months compared to the others
- A cross-hemisphere mode disrupts the development of the zonal wind anomalies and the discharge process in most prolonged events

Supporting Information:
- Supporting Information S1

Correspondence to:
C.-W. Lee,
f05229029@ntu.edu.tw

Citation:
Lee, C.-W., Tseng, Y.-H., Sui, C.-H., Zheng, F., & Wu, E.-T. (2020). Characteristics of the prolonged El Niño events during 1960–2020. *Geophysical Research Letters*, *47*, e2020GL088345. https://doi.org/10.1029/2020GL088345

Received 11 APR 2020
Accepted 10 MAY 2020
Accepted article online 13 MAY 2020

Abstract Most El Niño events decayed rapidly after boreal winter, while some events prolonged and grew again in the second year, accounting for 5 out of the 17 episodes during 1960–2020. In their development stages, warm water volume (WWV) anomalies were comparable to the other events, but the growth of sea surface temperature (SST) and westerly anomalies and the discharge of WWV were delayed by about a season. The weak but warm SST anomaly in Eastern Pacific persisted into next year, intensified again via Bjerknes feedback, and decayed after the second boreal winter. In June–October of 1968, 1986, 2014, and 2018, a strengthened cross-hemisphere SST gradient appeared in Eastern Pacific, induced anomalous southerly at the equator, and disrupted the zonal positive feedback. The intensity of this meridional mode is independent of the El Niño state and is weaker in late 1990s to early 2010s than in other decades.

Plain Language Summary An El Niño event seldom lasts for more than a year, but such prolonged events still account for 5 out of the 17 El Niño episodes in 1960–2020. The sea surface temperature (SST) anomaly of a warm event usually peaks in the boreal winter when the subsurface warm water volume (WWV) anomaly turns negative as discharged by an equatorial westerly wind anomaly. The preconditioned WWV amount of the prolonged events is similar to that in the common events, but the evolution of SST, wind, and WWV is slower. The Eastern Pacific SST anomaly increases again in the second year and decays rapidly after the second boreal winter. The delayed development results from disruption by a cross-hemisphere meridional SST dipole and the associated cross-equatorial wind. The SST dipole is unrelated to the ENSO and is weaker in late 1990s to early 2010s than in other decades.

1. Introduction

The El Niño-Southern Oscillation (ENSO) is an atmosphere-ocean coupled variability dominant over Tropical Pacific on the interannual timescale and has a profound impact on the global climate (e.g., Ropelewski & Halpert, 1987; Trenberth et al., 1998). The warm phase of ENSO (i.e., El Niño) usually follows an oceanic heat content initially piled up in equatorial Western Pacific (Wyrtki, 1975; see also Jin, 1997) and is often triggered by the westerly wind events (WWEs; e.g., Harrison & Vecchi, 1997). Most El Niño events mature in boreal winter and decay rapidly in the following spring. Its transition to the cold state (La Niña) results from several oceanic negative feedbacks, including upwelling equatorial Kelvin waves resulting from the Rossby waves reflected at the western Pacific (i.e., delayed oscillator; e.g., Suarez & Schopf, 1988), the meridional discharge of the basin-wide warm water volume (WWV; Jin, 1997; Li, 1997; Meinen & McPhaden, 2000), and the reversal of zonal heat transport due to the change of the meridional concavity of the thermocline structure (Chen et al., 2016).

The decay of El Niño can also be facilitated by oceanic upwelling Kelvin waves forced by equatorial easterly wind anomalies. The easterly anomalies are generated over equatorial Western Pacific as an anomalous anticyclonic circulation over subtropical western North Pacific, which is strengthened through the interaction between the local cold sea surface temperature (SST) anomalies (SSTA) and climatological northeasterly (Wang et al., 2000, 2001). The remote influences from Indian Ocean or Atlantic Ocean can also facilitate the decay of El Niño. In boreal autumn, when the positive phase of Indian ocean dipole SSTA is present, the westerly anomalies over Western Pacific are reinforced by the atmospheric cooling over the eastern Indian ocean; it enhances the upwelling equatorial Rossby waves that will rise equatorial thermocline depths after they are reflected at the western boundary in the following seasons

Table 1
The Classification of El Niño During 1960–2020 Based on Whether the Warm State Persists for One or Two Boreal Winter

One-winter El Niño (12 events)	Two-winter El Niño (5 events)
1963/1964, 1965/1966, 1972/1973, 1979/1980, 1982/1983, 1991/1992, 1994/1995, 1997/1998, 2002/2003, 2004/2005, 2006/2007, 2009/2010	1968/69/70, 1976/77/78, 1986/87/88, 2014/15/16, 2018/19/20

Note. See section 2 for detailed definition.

(Izumo et al., 2010, 2016). In boreal winter, the Indian ocean dipole is usually replaced by the basin-wide warming; therefore, the equatorial anomalous easterlies prevailing over the IO are favored to intrude into Western Pacific (Kug & Kang, 2006; Ohba & Ueda, 2007; Yamanaka et al., 2009). Additionally, the warming of Tropical North Atlantic (TNA; e.g., Nobre & Shukla, 1996) is a robust response in the boreal spring after El Niño matures (e.g., Enfield, 1996; Jiang & Li, 2019), while the warm SSTA over TNA can enhance the anomalous anticyclone over the western North Pacific (Li et al., 2017; Wang et al., 2017) and may trigger the cold phase of ENSO (Ham et al., 2013); the variability over TNA may play a role in the rapid decay of El Niño as well, but the detailed interactions require further studies.

The mechanisms for the fast decay of El Niño have been investigated by many studies, but less attention is paid to the processes responsible for prolonged duration of El Niño events, such as the 2014/2015/2016 event. In early 2014, a significant amount of WWV had accumulated over Western Pacific (McPhaden, 2015), and a series of WWEs occurred (Menkes et al., 2014); therefore, a major El Niño was predicted to mature in the 2014/2015 boreal winter (e.g., Tollefson, 2014). However, its growth was slow, and the magnitude in 2014/2015 winter was far below expectation. The warm condition extended into 2015/2016 winter. The stalled development was attributed to the pause of WWEs (Menkes et al., 2014), the easterly wind events in the 2014 summer (Hu & Fedorov, 2016; Levine & McPhaden, 2016), and the anomalous cross-equatorial southerlies (Wu et al., 2018) associated with the warm SSTA in the subtropical eastern North Pacific and the cold SSTA in the subtropical eastern South Pacific (Min et al., 2015; Zhu et al., 2016).

Although this prolonged type of El Niño occurs less frequently than the common El Niño or prolonged La Niña (Kessler, 2002; Larkin & Harrison, 2002), it still accounts for 5 out of the 17 El Niño events in 1960–2020 (Table 1). These events would be referred to as the prolonged or two-winter El Niño interchangeably in this study. Although their occurrence likely results from random reasons, we will show some common features they share and propose a possible interaction between developing ENSO and a cross-hemisphere meridional SST dipole over Eastern Pacific.

2. Data and Methods

The National Oceanic and Atmospheric Administration (NOAA) Extended Reconstructed Sea Surface Temperature Version 5 (ERSSTv5; Huang et al., 2017) monthly SST for a global 2° × 2° grid from 1854 to present is employed. The monthly 850-hPa wind data are retrieved from the European Centre for Medium Range Weather Forecast (ECMWF) reanalysis-40 (ERA-40; Uppala et al., 2005) at 2.5° × 2.5° grid for 1957–2002 and from ECMWF reanalysis-5 (ERA-5; Hersbach & Dee, 2016) at 0.25° × 0.25° for 1979–2020. Simple Ocean Data Assimilation Version 2.2.4 (SODA-v2.2.4; Giese & Ray, 2011) at 0.5° × 0.5° grid from 1950–2010 and National Center for Environment Prediction (NCEP) Global Ocean Data Assimilation System (GODAS; Behringer & Xue, 2004) at 1/3° × 1° (higher latitudinal resolution) are used for oceanic subsurface temperature.

Data of different periods are first merged. The wind data from ERA-5 are regridded to the coarser 2.5° × 2.5° grid as ERA-40, and the data are concatenated after an arithmetic mean is applied to the overlapping period, January 1979 to August 2002. The 20°C isotherm depth (D20) is derived in SODA-v2.2.4 and GODAS separately, before D20 is interpolated to a coarser 0.5° × 1° grid; they are merged in time, and an arithmetic mean value is used during the overlapping period, 1980–2010.

A moving 31-year centered window monthly mean is subtracted to calculate the monthly anomalies, and a 3-month running mean is applied to suppress intraseasonal signals. The result does not change significantly if an 11-year window is used instead. The WWV is defined as the integrated volume above D20 over 5°N to 5°S, 120°E to 80°W, following the analysis of Meinen and McPhaden (2000). A zonal wind index is derived as the area-averaged 850-hPa zonal wind over 5°N to 5°S, 135°E to 120°W for Pacific basin, according to the trade wind index defined by Climate Prediction Center (CPC). The Oceanic Niño Index (ONI) is the

3-month running mean of Niño3.4 (5°S to 5°N, 170–120°W) SSTA. Following the CPC definition, an El Niño event is defined when the ONI is above 0.5°C for five consecutive overlapping 3-month periods.

If the El Niño criteria is met, and the ONI stays above zero and exceeds 0.5°C again in the following boreal winter (November-December-January), it is defined as a two-winter El Niño; otherwise, the El Niño persistent for only one winter is classified as the one-winter type. The ongoing 2018/2019/2020 is considered a two-winter event. From 1960 to 2020, 5 out of 17 events are categorized as the two-winter type. The first, second, and third year of each event will be referred to as year(0), year(1), and year(2), respectively.

3. Results

First, the evolution of two-winter El Niño will be documented. Both one-winter and two-winter types of El Niño have a higher-than-average WWV during their development (Figure 1), while other features are distinct. The evolution of each field in the first year is about one season later compared to the one-winter El Niño composite. The ONI reaches the 0.5°C threshold late by about 3 months, and the accompanied anomalous westerly is relatively weak in the first year; the time of WWV anomaly turning negative is also about one season later. In addition, the ONI increases again in the second year although the basin wide WWV anomaly is nearly zero or negative. After reaching the second peak, the two-winter event rapidly decays to the cold state like the one-winter El Niño.

In the one-winter event composite, the anomalous westerly first appears west of the dateline (Figure S1f in the supporting information) and propagates eastward as the warm SSTA over Eastern Pacific strengthens (Figure S2f). In balance with the anomalous westerly wind stress, the thermocline over western Pacific is raised, and the basin mode transitions into a tilting mode in September(0)-November(0) (Figure S3f), while the basin-integrated WWV is discharged and decreases. The shallower D20 anomaly propagates eastward, and the SSTA decays quickly below 0.5°C in March(1)-May(1) of the one-winter events.

The equatorial warm SSTA of the two-winter events emerges from Central Pacific in January(0) and extends eastward afterward except for 1976/1977/1978, in which the warm SSTA develops from the eastern coast (Figure S2). The westerly anomaly also follows the eastward extension of the SSTA with a magnitude weaker than that in the one-winter events; while the anomalous westerly is weak in the first year, it persists into the second year (Figure S1). The D20 anomaly shows a basin-wide deepened mode as in January(0)-April(0) of the two-winter events (Figure S3), but the tilting mode is not prominent until January(1) because the anomalous westerly is weak. As a result, the equatorial Eastern Pacific thermocline remains deepened, maintains the weak but warm SSTA through March(1)-May(1), and triggers the positive Bjerknes feedback in the second boreal summer and autumn for the SSTA to grow again despite zero or negative basin-wide WWV anomaly (Figure 1). Afterward, the shallower D20 signals extend to Eastern Pacific, and the event terminates rapidly like the one-winter type. The 1976/1977/1978 event does not share most common features of the rest two-winter events; it co-occurs with the cold-to-warm phase transition of Interdecadal Pacific Oscillation (IPO; Power et al., 1999), and its SSTA distribution in December(0)-January-February(1) resembles the broad meridional extent of a warm IPO phase (Figure S4).

Next, the reason for the late development of two-winter El Niño is investigated. For one-winter El Niño, in June(0)-October(0), the warm SSTA symmetric about the equator dominates Eastern Pacific, and the equatorial wind anomaly is prevailed by westerly (Figure 2). In comparison, except for 1976/1977/1978, a warm SSTA extends southwestward from subtropical North Pacific to the equatorial dateline (Figure 2), indicating that the two-winter events might be triggered by the "seasonal footprinting mechanism" (Vimont et al., 2003; see also Tseng et al., 2017); therefore, the equatorial warm SSTA signal emerges from Central Pacific in Figure S2. There is also a cold SSTA over subtropical eastern South Pacific slightly weaker than the north warm one; they form a meridional dipole (boxes in Figure 2), and the wind anomaly converges over the subtropical eastern North Pacific of warm SSTA. Meanwhile, a cross-equatorial southerly is driven around this longitudinal band; it could continue for several months and persist into January(1) (Figure S5). The seasonal cross-equatorial wind is prevailed by southerly in June–October over 180° to 140°W, when the meridional component of convergence in the northern tropics is the strongest (Figure S6), indicating the seasonal activity of Inter-Tropical Convergence Zone (ITCZ). The meridional component of anomalous wind in June(0)-October(0) of the one-winter El

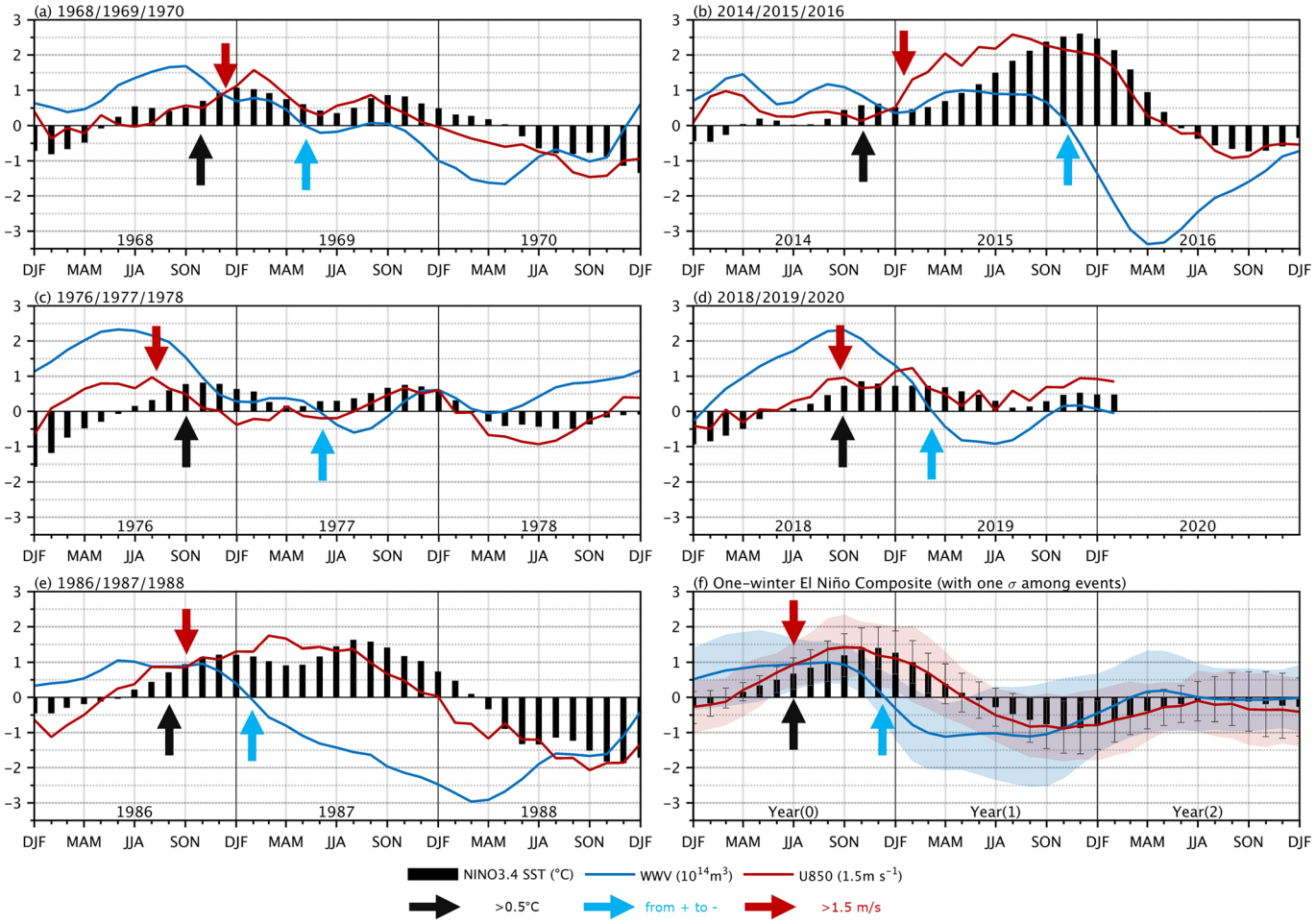

Figure 1. The evolution of anomalous Niño3.4 SST (°C; black), WWV (10^{14} m^3; blue), and 850-hPa zonal wind index (1.5 m s^{-1}; red) in (a) 1968/1969/1970, (b) 2014/2015/2016, (c) 1976/1977/1978, (d) 2018/2019/2020, (e) 1986/1987/1988 El Niño, and (f) one-winter event composite. The black, blue, and red arrows, respectively, denote when Niño3.4 SSTA reaches 0.5°C, WWV turns negative, and zonal wind index exceeds 1.5 m s^{-1}. The error bar and shading area in (f) represent +/−1 standard deviation of each variable among one-winter El Niño events.

Niño composite is weak northerly (Figure S5f), suggesting that the ITCZ is slightly displaced equatorward due to the equatorially symmetric warm SSTA, in favor of the Bjerknes feedback; in contrast, an anomalous southerly appears in the two-winter events (Figure S5). This meridional dipole may disrupt the zonal positive feedback in the El Niño development.

The intensity of this dipole is defined as the areal averaged SSTA over 170–120°W, 16–4°N minus that over 170–120°W, 4–16°S in June–October (Figure 3a); the result does not change significantly if a slightly larger or smaller region is chosen. All the four El Niño events developing with the meridional SST dipole of intensity above 0.2°C are prolonged type (Figure 3a), while the rest events are one-winter events, except for 1976/1977/1978. The strength of June–October SSTA dipole barely changes with the removal of the regression on Niño3.4 SSTA in the previous December–February, the concurrent June–October, or the following December–February; also, an El Niño event can occur during an either positive or negative state of the meridional mode (Figure 3a). This suggests that this meridional mode is unrelated to the ENSO, as the pattern of the latter is mostly symmetric about the equator (Figures 3b–3d). The SST dipole varies on not only interannual but also decadal timescales (Figure 4). Without removal of a moving 31-year centered window climatology, the absolute intensity of the meridional SST dipole is steady at about +0.4°C from 1960s to 1980s, but a weakening trend shows in early 1990s to late 2000s, followed by a strengthening trend afterward. The

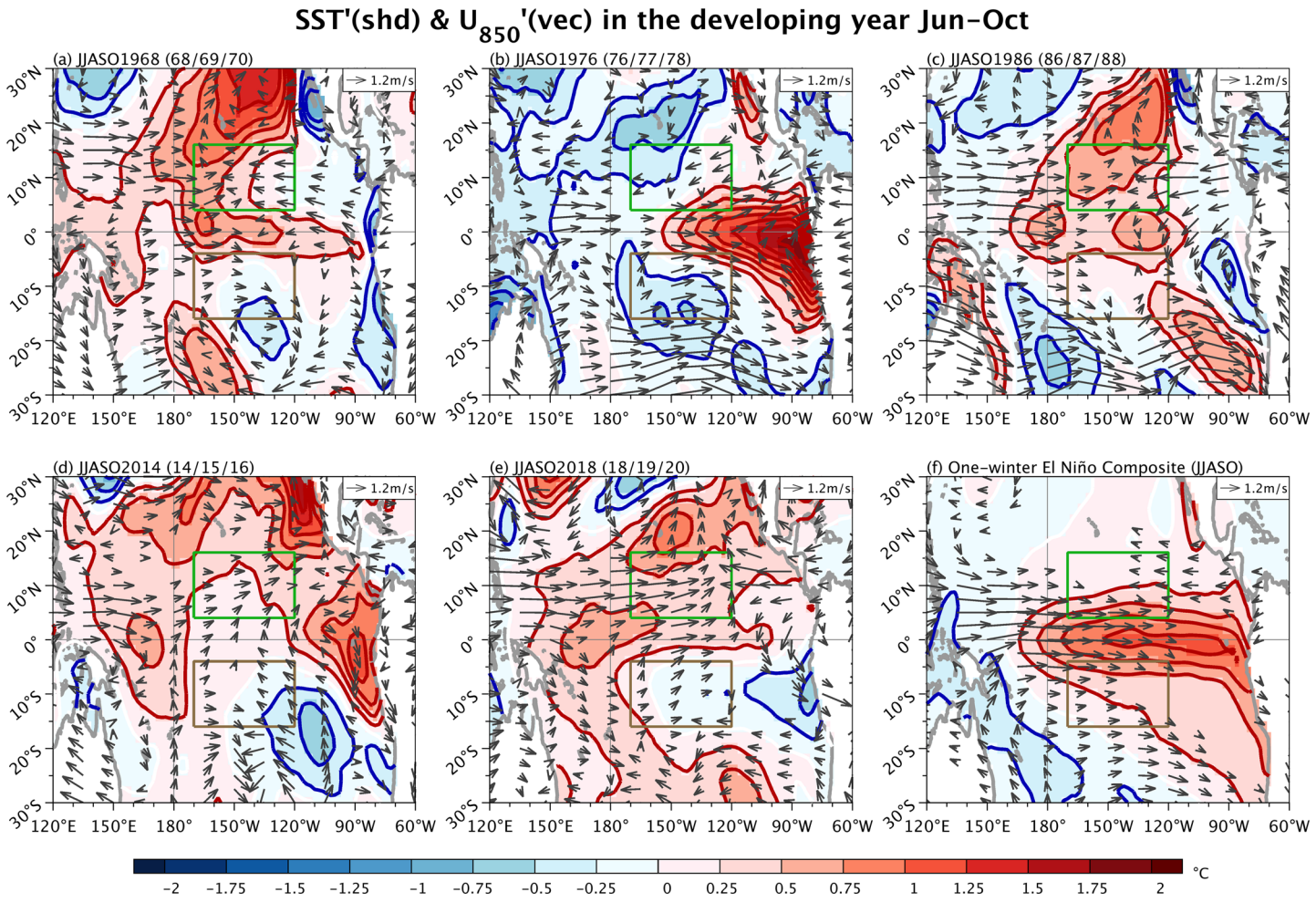

Figure 2. The SST (shading) and 850-hPa wind (vectors) anomalies in the June–October of developing year in (a) 1968/1969/1970, (b) 1976/1977/1978, (c) 1986/1987/1988, (d) 2014/2015/2016, (e) 2018/2019/2020 El Niño, and (f) one-winter event composite. The green and brown boxes denote the location of 170–120°W, 16–4°N and 170–120°W, 4–16°S, respectively, for the definition of the SST dipole intensity.. The minimum vector shown is 0.4 m s^{-1}.

intensity in early 1990s to early 2010s is about 0.2°C weaker than that in other decades during which the four two-winter events occur.

4. Discussion

The two-winter El Niño events evolve more slowly than the one-winter type, and a meridional mode is involved in the stalled development except for 1976/1977/1978. The Niño3.4 SSTA reaches the first peak around December(0) and grows again in the middle of the second year (Figure 1), possibly because the seasonal-dependent thermodynamic damping is stronger in boreal spring (Dommenget & Yu, 2016) and the atmosphere-ocean coupling is more unstable in boreal summer and autumn (Stein et al., 2010; Tziperman et al., 1997). The meridional dipole SST can inhibit the growth of El Niño in both atmospheric and oceanic dynamics. The enhanced ITCZ activity in the north can suppress the equatorial convection anomaly via a meridional overturning circulation. In the ocean, the westward component of the northwestward current induced by the cross-equatorial southerly in the Southern Hemisphere can cool the SST through negative zonal and vertical advection anomalies, while the northward component can transport subtropical cold water to the equator (Wu et al., 2018). Hence, the SST and atmospheric anomalies grow slowly despite an anomalously high WWV.

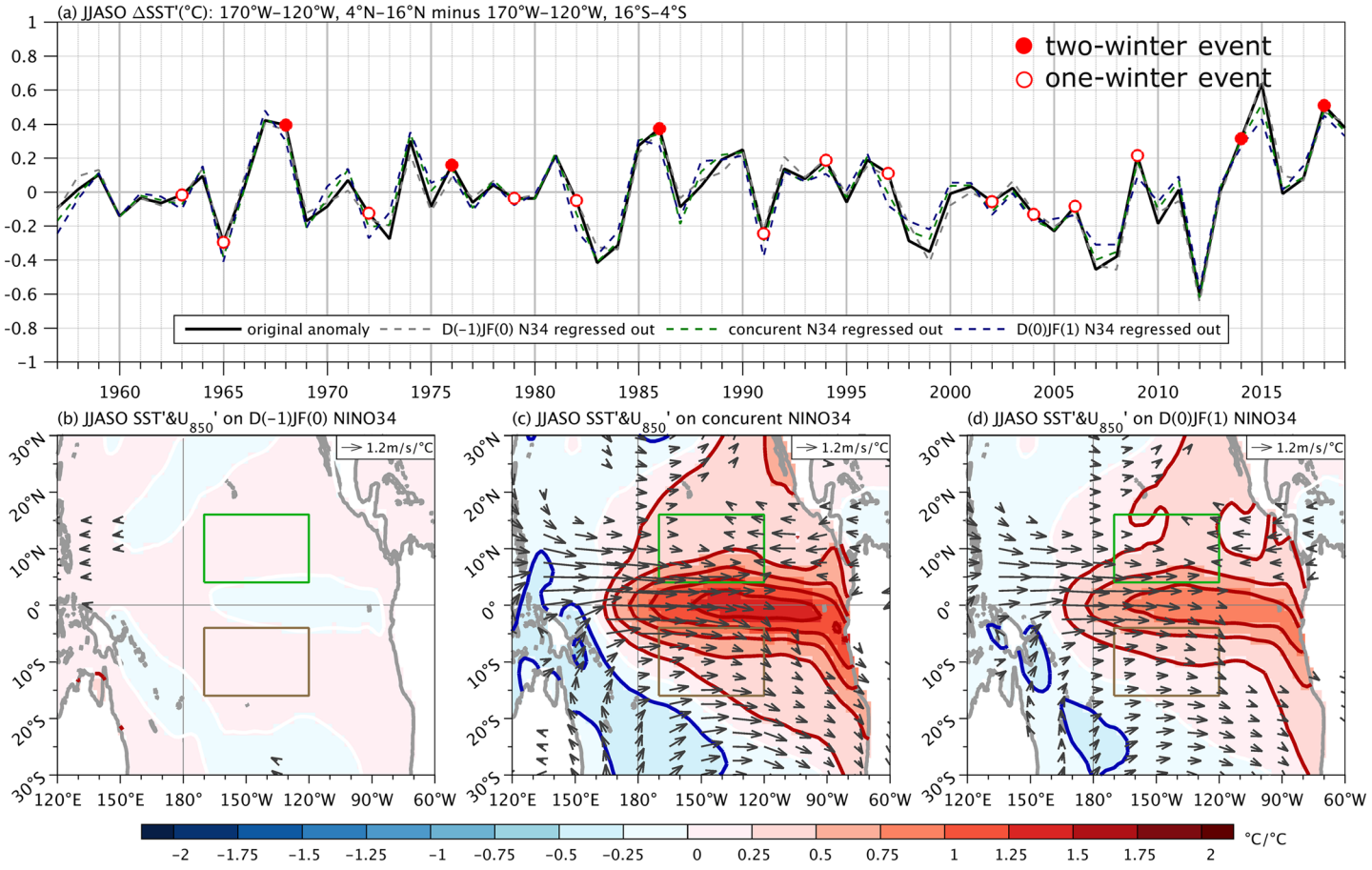

Figure 3. (a) The area-averaged interannual SSTA difference in June–October between 16–4°N and 4–16°S over 170–120°W (solid). The closed (open) circles denote the developing year of two-winter (one-winter) El Niño events. The gray, green, and blue dashed lines, respectively, represent the SSTA difference with regression on the previous December–February, the concurrent, and the following December–February Niño3.4 SSTA removed. (b–d) The regression of SST (shading) and 850-hPa wind (vectors) anomalies on (b) the previous December–February, (c) the concurrent June–October, and (d) the following December–February Niño3.4 SSTA. The minimum vector shown is 0.4 m s^{-1} °C^{-1}.

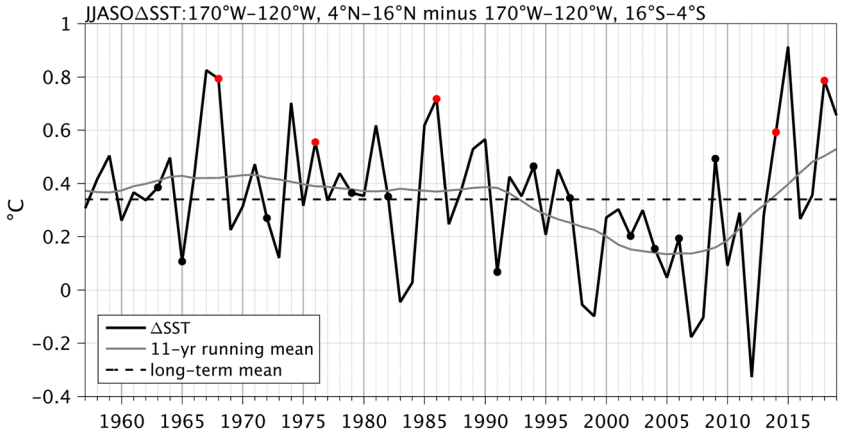

Figure 4. The June–October SST difference between 170–120°W, 16–4°N and 170–120°W, 4–16°S (black solid); its 11-year running average (gray solid); and the 1957–2019 mean (dashed). The red (black) circle marks the developing year of two-winter (one-winter) events.

Although there are some common characteristics, the two-winter events are still quite different from one another. For example, 1976/1977/1978 happens with the phase transition of the IPO; 1968/1969/1970 and 1986/1987/1988 show an abnormal phase locking to seasonal cycle, peaking in September–November 1969 and July–September 1987, respectively; 2014/2015/2016 is one of the strongest El Niño events, while 2018/2019/2020 is accompanied by a record-breaking positive IOD event in 2019. The meridional mode can partially contribute to the occurrence of two-winter El Niño, but the evolution of two-winter events might largely be a result of stochastic forcings such as weather events or variability in the remote basins.

The meridional SST dipole may also influence the duration of La Niña events in a similar way; for instance, 1973/1974/1975/1976, 1983/1984/1985, 1998/1999/2000/2001, and 2007/2008/2009 prolonged La Niña events occurs with a relatively strong negative dipole in June–October of the first year (Figure 3). When the SSTA dipole intensity is negative, the ITCZ may be displaced equatorward from the Northern Hemisphere, favoring a westerly anomaly over Western-Central Pacific, which can counteract the positive feedback of a developing La Niña. As the development is delayed, the recharging of WWV by easterly may not be enough for a phase transition in the coming year so an event continues.

The cross-equatorial SST gradient is a robust unstable atmosphere-ocean coupled mode in annual cycle, maintained by wind-upwelling-SST feedback (Chang & Philander, 1994), wind-evaporation-SST feedback (Xie & Philander, 1994), and stratocumulus-radiation-SST feedback (Li & Philander, 1996). The processes maintaining the SST dipole could also operate on interannual time scales (Xie et al., 2018). Hu and Fedorov (2018) showed an increasing trend of cross-equatorial southerly over Eastern Pacific; consistently, the interannual cross-equatorial southerly anomaly was relatively stronger in 2014 and 2018 but slightly weaker in 1986 (Figure 2), and the SST dipole shows an increasing trend after late 2000s (Figure 4). How the SSTA dipole generally influences the ENSO evolution, what initially triggers the SSTA dipole for two-winter El Niño, and whether the occurrence of two-winter El Niño follows decadal variability need further investigation.

5. Conclusions

El Nino events are classified into one-winter and two-winter (prolonged) types based on the duration of warm phase. The warm state sustains for only one boreal winter in the one-winter El Niño events while it persists into another boreal winter (November–January) in the two-winter type. Five out of the 17 El Nino events in 1960–2020 are two-winter type (Table 1).

Although these events show different evolutions and are likely to occur for different reasons, there are still some similar characteristics. Compared to one-winter El Niño, prolonged shows a delayed development by about a season (Figure 1). The late development causes insufficient discharge of WWV; the SSTA is maintained by the deepened thermocline in equatorial Eastern Pacific (Figure S3), and it grows again in the following boreal summer when season-dependent atmosphere-ocean coupling is more unstable.

A strengthened cross-hemisphere SST gradient in subtropical Eastern Pacific during June–October might play an important role in the delayed El Niño development (Figure 2), except for the 1976/1977/1978 event when the IPO turned from cold to warm phase. The SSTA dipole induces cross-equatorial southerly, enhances the ITCZ activity in the north, and disrupts the Bjerknes feedback that requires equatorial zonal coupling. All the four El Niño events developing with the intensity of the meridional mode above 0.2°C are two-winter type (Figure 3). The SST dipole varies independently of the state of ENSO (Figure 3) and shows a decadal variation that is lower in late 1990s to early 2010s than in other decades when the two-winter El Niño occurs (Figure 4).

Data Availability Statement

All data used in this study can be publicly downloaded online. The European Centre for Medium-Range Weather Forecasts (ECMWF) ReAnalysis-40 (ERA-40) can be found in the CGD website (http://www.cgd.ucar.edu/cas/catalog/reanalysis/ecmwf/era40/index.html), and ReAnalysis-5 (ERA-5) can be found in the CDS website (https://cds.climate.copernicus.eu/cdsapp#!/dataset/reanalysis-era5-pressure-levels-monthly-means). The Simple Ocean Data Assimilation (SODA) data are retrieved from the National Center for

Atmospheric Research website (https://climatedataguide.ucar.edu/climate-data/soda-simple-ocean-data-assimilation). The National Centers for Environment Prediction (NCEP) Global Ocean Data Assimilation System (GODAS) data can be found online (from https://cfs.ncep.noaa.gov/cfs/godas/monthly/).

Acknowledgments
Chung-Hsiung Sui was supported by the MOST, Taiwan, Grant 108-2111-M-002-016. Yu-heng Tseng was supported by the MOST, Taiwan, Grant 107-2611-M-002-013-MY4. Fei Zheng was supported by the Strategic Priority Research Program of the Chinese Academy of Sciences, Grant XDB42000000. The comments from two anonymous reviewers are appreciated.

References

Behringer, D. W., & Xue, Y. (2004). Evaluation of the global ocean data assimilation system at NCEP: The Pacific Ocean, Paper 2.3 presented at eighth symp. On integrated observing and assimilation systems for atmosphere, oceans, and land surface, am. Meteorol. Soc., Seattle, Wash., Preprints. [Available at https://ams.confex.com/ams/84Annual/techprogram/paper_70720.htm]

Chang, P., & Philander, S. G. (1994). A coupled ocean-atmosphere instability of relevance to the seasonal cycle. *Journal of the Atmospheric Sciences*, *51*(24), 3627–3648. https://doi.org/10.1175/1520-0469(1994)051<3627:acoior>2.0.co;2

Chen, H. C., Hu, Z. Z., Huang, B., & Sui, C. H. (2016). The role of reversed equatorial zonal transport in terminating an ENSO event. *Journal of Climate*, *29*(16), 5859–5877. https://doi.org/10.1175/JCLI-D-16-0047.1

Dommenget, D., & Yu, Y. (2016). The seasonally changing cloud feedbacks contribution to the ENSO seasonal phase-locking. *Climate Dynamics*, *47*(12), 3661–3672. https://doi.org/10.1007/s00382-016-3034-6

Enfield, D. B. (1996). Relationships of inter-American rainfall to tropical Atlantic and Pacific SST variability. *Geophysical Research Letters*, *23*(23), 3305–3308. https://doi.org/10.1029/96GL03231

Giese, B. S., & Ray, S. (2011). El Niño in simple ocean data assimilation (SODA), 1781–2008. *Journal of Geophysical Research*, *116*(C2), C02024. https://doi.org/10.1029/2010JC006695

Ham, Y. G., Kug, J. S., Park, J. Y., & Jin, F. F. (2013). Sea surface temperature in the north tropical Atlantic as a trigger for El Niño/Southern Oscillation events. *Nature Geoscience*, *6*(2), 112–116. https://doi.org/10.1038/ngeo1686

Harrison, D. E., & Vecchi, G. A. (1997). Westerly wind events in the tropical pacific, 1986-95. *Journal of Climate*, *10*(12), 3131–3156. https://doi.org/10.1175/1520-0442(1997)010<3131:WWEITT>2.0.CO;2

Hersbach, H., & Dee, D. (2016). *ERA5 reanalysis is in production, ECMWF Newsletter **147***. Reading, UK: ECMWF. [Retrieved from https://www.ecmwf.int/en/newsletter/147/news/era5-reanalysis-production

Hu, S., & Fedorov, A. V. (2016). Exceptionally strong easterly wind burst stalling El Niño of 2014. *Proceedings of the National Academy of Sciences*, *113*(8), 2005–2010. https://doi.org/10.1073/pnas.1514182113

Hu, S., & Fedorov, A. V. (2018). Cross-equatorial winds control El Niño diversity and change. *Nature Climate Change*, *8*(9), 798–802. https://doi.org/10.1038/s41558-018-0248-0

Huang, B., Thorne, P. W., Banzon, V. F., Boyer, T., Chepurin, G., Lawrimore, J. H., et al. (2017). Extended Reconstructed Sea Surface Temperature, Version 5 (ERSSTv5): Upgrades, validations, and intercomparisons. *Journal of Climate*, *30*(20), 8179–8205. https://doi.org/10.1175/JCLI-D-16-0836.1

Izumo, T., Vialard, J., Dayan, H., Lengaigne, M., & Suresh, I. (2016). A simple estimation of equatorial pacific response from windstress to untangle Indian ocean dipole and basin influences on El Niño. *Climate Dynamics*, *46*(7-8), 2247–2268. https://doi.org/10.1007/s00382-015-2700-4

Izumo, T., Vialard, J., Lengaigne, M., DeBoyer Montegut, C., Behera, S. K., Luo, J. J., et al. (2010). Influence of the state of the Indian Ocean Dipole on the following years El Niño. *Nature Geoscience*, *3*(3), 168–172. https://doi.org/10.1038/ngeo760

Jiang, L., & Li, T. (2019). Relative roles of El Niño-induced extratropical and tropical forcing in generating Tropical North Atlantic (TNA) SST anomaly. *Climate Dynamics*, *53*(7-8), 3791–3804. https://doi.org/10.1007/s00382-019-04748-7

Jin, F.-F. (1997). An equatorial ocean recharge paradigm for ENSO. Part I: Conceptual Model Pacific from his analysis of the empirical relations of. *Journal of the Atmospheric Sciences*, *54*, 811–829. https://doi.org/10.1175/1520-0469(1997)054<0811:AEORPF>2.0.CO;2

Kessler, W. S. (2002). Is ENSO a cycle or a series of events? *Geophysical Research Letters*, *29*(23), 2125. https://doi.org/10.1029/2002gl015924

Kug, J. S., & Kang, I. S. (2006). Interactive feedback between ENSO and the Indian Ocean. *Journal of Climate*, *19*(9), 1784–1801. https://doi.org/10.1175/JCLI3660.1

Larkin, N. K., & Harrison, D. E. (2002). ENSO warm (El Niño) and cold (La Niña) event life cycles: Ocean surface anomaly patterns, their symmetries, asymmetries, and implications. *Journal of Climate*, *16*, 1118–1140. https://doi.org/10.1175/1520-0442(2002)015<1118:EWENOA>2.0.CO;2

Levine, A. F. Z., & McPhaden, M. J. (2016). How the July 2014 easterly wind burst gave the 2015–2016 El Niño a head start. *Geophysical Research Letters*, *43*, 6503–6510. https://doi.org/10.1002/2016GL069204

Li, T. (1997). Phase transition of the El Niño-Southern Oscillation: A stationary SST mode. *Journal of the Atmospheric Sciences*, *54*(24), 2872–2887. https://doi.org/10.1175/1520-0469(1997)054<2872:ptoten>2.0.co;2

Li, T., & Philander, S. G. H. (1996). On the annual cycle of the eastern equatorial Pacific. *Journal of Climate*, *9*(12), 2986–2998. https://doi.org/10.1175/1520-0442(1996)009<2986:OTACOT>2.0.CO;2

Li, T., Wang, B., Wu, B., Zhou, T., Chang, C. P., & Zhang, R. (2017). Theories on formation of an anomalous anticyclone in western North Pacific during El Niño: A review. *Journal of Meteorological Research*, *31*(6), 987–1006. https://doi.org/10.1007/s13351-017-7147-6

McPhaden, M. J. (2015). Playing hide and seek with El Niño. *Nature Climate Change*, *5*(9), 791–795. https://doi.org/10.1038/nclimate2775

Meinen, C. S., & McPhaden, M. J. (2000). Observations of warm water volume changes in the equatorial Pacific and their relationship to El Nino and La Nina. *Journal of Climate*, *13*(20), 3551–3559. https://doi.org/10.1175/1520-0442(2000)013<3551:OOWWVC>2.0.CO;2

Menkes, C. E., Lengaigne, M., Vialard, J., Puy, M., Marchesiello, P., Cravatte, S., & Cambon, G. (2014). About the role of Westerly Wind Events in the possible development of an El Niño in 2014. *Geophysical Research Letters*, *41*, 6476–6483. https://doi.org/10.1002/2014GL061186

Min, Q., Su, J., Zhang, R., & Rong, X. (2015). What hindered the El Niño pattern in 2014? *Geophysical Research Letters*, *42*, 6762–6770. https://doi.org/10.1002/2015GL064899

Nobre, P., & Shukla, J. (1996). Variations of sea surface temperature, wind stress, and rainfall over the tropical Atlantic and South America. *Journal of Climate*, *9*(10), 2464–2479. https://doi.org/10.1175/1520-0442(1996)009<2464:VOSSTW>2.0.CO;2

Ohba, M., & Ueda, H. (2007). An impact of SST anomalies in the Indian Ocean in acceleration of the El Niño to La Niña transition. *Journal of the Meteorological Society of Japan*, *85*(3), 335–348. https://doi.org/10.2151/jmsj.85.335

Power, S., Casey, T., Folland, C., Colman, A., & Mehta, V. (1999). Inter-decadal modulation of the impact of ENSO on Australia. *Climate Dynamics*, *15*(5), 319–324. https://doi.org/10.1007/s003820050284

Ropelewski, C. F., & Halpert, M. S. (1987). Global and regional scale precipitation patterns associated with the El Niño/Southern Oscillation. *Monthly Weather Review*, *115*(8), 1606–1626. https://doi.org/10.1175/1520-0493(1987)115<1606:GARSPP>2.0.CO;2

Stein, K., Schneider, N., Timmermann, A., & Jin, F. F. (2010). Seasonal synchronization of ENSO events in a linear stochastic model. *Journal of Climate*, *23*(21), 5629–5643. https://doi.org/10.1175/2010JCLI3292.1

Suarez, M. J., & Schopf, P. S. (1988). A delayed action oscillator for ENSO. *Journal of the Atmospheric Sciences*, *45*(21), 3283–3287. https://doi.org/10.1175/1520-0469(1988)045<3283:adaofe>2.0.co;2

Tollefson, J. (2014). El Niño tests forecasters. *Nature*, *508*(7494), 20–21. https://doi.org/10.1038/508020a

Trenberth, K. E., Branstator, G. W., Karoly, D., Kumar, A., Lau, N.-C., & Ropelewski, C. (1998). Progress during TOGA in understanding and modeling global teleconnections associated with tropical sea surface temperatures. *Journal of Geophysical Research*, *103*(C7), 14291–14324. https://doi.org/10.1029/97jc01444

Tseng, Y. H., Ding, R., & Huang, X. M. (2017). The warm Blob in the northeast Pacific—The bridge leading to the 2015/16 El Niño. *Environmental Research Letters*, *12*(5), 054019. https://doi.org/10.1088/1748-9326/aa67c3

Tziperman, E., Zebiak, S. E., & Cane, M. A. (1997). Mechanisms of seasonal-ENSO interaction. *Journal of the Atmospheric Sciences*, *54*(1), 61–71. https://doi.org/10.1175/1520-0469(1997)054<0061:mosei>2.0.co;2

Uppala, S. M., KÅllberg, P. W., Simmons, A. J., Andrae, U., Da Costa Bechtold, V., Fiorino, M., et al. (2005). The ERA-40 re-analysis. *The Quarterly Journal of the Royal Meteorological Society*, *131*(612), 2961–3012. https://doi.org/10.1256/qj.04.176

Vimont, D. J., Wallace, J. M., & Battisti, D. S. (2003). The seasonal footprinting mechanism in the Pacific: Implications for ENSO. *Journal of Climate*, *16*(16), 2668–2675. https://doi.org/10.1175/1520-0442(2003)016<2668:TSFMIT>2.0.CO;2

Wang, B., Wu, R., & Fu, X. (2000). Pacific-East Asian teleconnection: How does ENSO affect east Asian climate? *Journal of Climate*, *13*(9), 1517–1536. https://doi.org/10.1175/1520-0442(2000)013<1517:PEATHD>2.0.CO;2

Wang, B., Wu, R., Lukas, R., & An, S.-I. (2001). A possible mechanism for ENSO turnabout. In IAP/Academia Sinica (Ed.), *Dynamics of Atmospheric General Circulation and Climate* (pp. 552–578). Beijing: China Meteorological Press. [Available from http://www.soest.hawaii.edu/MET/Faculty/bwang/bw/paper/wang80.pdf

Wang, L., Yu, J. Y., & Paek, H. (2017). Enhanced biennial variability in the Pacific due to Atlantic capacitor effect. *Nature Communications*, *8*(1), 14,887. https://doi.org/10.1038/ncomms14887

Wu, Y. K., Chen, L., Hong, C. C., Li, T., Chen, C. T., & Wang, L. (2018). Role of the meridional dipole of SSTA and associated cross-equatorial flow in the tropical eastern Pacific in terminating the 2014 El Niño development. *Climate Dynamics*, *50*(5-6), 1625–1638. https://doi.org/10.1007/s00382-017-3710-1

Wyrtki, K. (1975). El Niño—The dynamic response of the equatorial Pacific Ocean to atmospheric forcing. *Journal of Physical Oceanography*, *5*(4), 572–584. https://doi.org/10.1175/1520-0485(1975)005<0572:ENTDRO>2.0.CO;2

Xie, S. P., Peng, Q., Kamae, Y., Zheng, X. T., Tokinaga, H., & Wang, D. (2018). Eastern pacific ITCZ dipole and ENSO diversity. *Journal of Climate*, *31*(11), 4449–4462. https://doi.org/10.1175/JCLI-D-17-0905.1

Xie, S. P., & Philander, S. G. H. (1994). A coupled ocean-atmosphere model of relevance to the ITCZ in the eastern Pacific. *Tellus*, *46*(4), 340–350. https://doi.org/10.3402/tellusa.v46i4.15484

Yamanaka, G., Yasuda, T., Fujii, Y., & Matsumoto, S. (2009). Rapid termination of the 2006 El Nino and its relation to the Indian Ocean. *Geophysical Research Letters*, *36*, L07702. https://doi.org/10.1029/2009GL037298

Zhu, J., Kumar, A., Huang, B., Balmaseda, M. A., Hu, Z. Z., Marx, L., & Kinter, J. L. (2016). The role of off-equatorial surface temperature anomalies in the 2014 El Niño prediction. *Scientific Reports*, *6*(1), 19,677. https://doi.org/10.1038/srep19677